Identification of Driver Braking Intention Based on Long Short-Term Memory (LSTM) Network

SHU WANG, XUAN ZHAO, QIANG YU, AND TIAN YUAN

School of Automobile, Chang'an University, Xi'an 710064, China

Corresponding author: Xuan Zhao (zhaoxuan@chd.edu.cn)

ABSTRACT Driving intention identification is a key technology which can improve the adaptability of the intelligent driver assistance systems and the energy efficiency of electric vehicles. This article proposes a novel method for identifying the driver braking intention. In order to improve the identification accuracy of driving intention, a braking intention identification model based on Long Short-Term Memory (LSTM) Network is constructed. The data of slight braking, normal braking and hard braking that can use for offline training are obtained through tests on real vehicle at Chang'an University vehicle performance testing ground. Support vector machine - recursive feature elimination (SVM-RFE) algorithm is used to select the characteristic parameter of braking intention identification model. The random search is subsequently used to optimize the hyper-parameters of LSTM. LSTM-based and Gaussian Hidden Markov Model (GHMM)-based model under different time window are used to identify braking intention of slight braking, normal braking and hard braking respectively. The results show that the Precision, Recall, F-measure, Accuracy of the braking intention identification model which propose in this paper based on LSTM are better than that of the braking intention identification model based on GHMM. Moreover, the Recall and Accuracy of the LSTM-based braking intention identification models are above 0.95, indicating the good ability of intention identification.

INDEX TERMS Braking intention recognition, driving safety, driver assistance system, LSTM network, accuracy and real-time.

I. INTRODUCTION

With the increasing complexity of road traffic environment, advanced driver assistance systems have been widely researched and deployed to avoid or mitigate collision, improve driving safety, and reduce accidents and fatalities [1]–[4]. As more intelligent driver assistants, in order to avoid the occurrence of false interventions and mismatch situations, and increase the driver's adaptability and trust to the vehicle, these systems should effectively obtain the driver's intentions [5]–[7]. At the same time, driving intentions have also been used in the electro-hydraulic composite braking control system of electric vehicles in order to improve braking safety, energy utilization and increase driving range [8]–[11]. When slight braking is recognized, braking force is generated only by the motor regenerative braking system to increase

energy utilization. When emergency braking is recognized, ABS and the motor regenerative braking system work in coordination to achieve braking safety. When the normal braking is recognized, the motor regenerative braking system and the mechanical hydraulic braking system work in coordination [12]–[15]. Therefore, in order to maximize the safety and energy utilization of electric vehicles, the braking intention also needs to be identified accurately and timely.

Various identification methods have been proposed to study on driving intentions of lane-changing, steering, starting, parking, and braking. HMM, as a kind of dynamic information processing method based on time-series cumulative probability, has been widely used. Pentland and Liu built a lane changing driving intention identification model based on Hidden Markov Model (HMM), and recognition accuracy reached 95% [16]. On the basis of Pentland and Liu, Oliver and Pentland also proposed the driving intention identification model based on coupled HMM. The recognition

---

The associate editor coordinating the review of this manuscript and approving it for publication was Shaohua Wan.

accuracy is 100% of passing and stop intentions, 85.7% of right lane change intention, 66.7% of left lane change intention, and 83.3% of start intention [17]. Tran and Sheng proposed a driver's intention prediction model using HMM and 6 maneuvers. The recognition accuracy is above 82% [18]. Li and Wang proposed a lane changing intention recognition model combining HMM and Bayesian filtering (BF), and recognition accuracy reached over 90.98% [19]. Zhao and Wang combined GHMM and GGAP-RBF for identifying driving intention, such as turning intention and braking intention [20], [21].

Fuzzy reasoning, support vector machine (SVM), artificial neural network (ANN) and hidden Markov model (HMM) are the also the primary methods employed in the field of driver intention recognition all over the world. Peng and Guo proposed a lane-changing classification method based on back-propagation neural network model, and recognition accuracy reached 85.44% [22]. Hua and Jiang proposed a driver's steering intention identification method using principal component analysis (PCA) [23]. Li and Zhu built a driver's starting intention identification method based on an artificial error back-propagation neutral network [24]. Kim and Bong proposed a lane change driving intention classification method using support vector machine (SVM). The recognition accuracy is greater than 90% [25]. Bocklisch proposed a lane change driving intention detection method using adaptive fuzzy pattern classification, and recognition accuracy reached over 86.3% [26]. Kim proposed a braking intention identification model using neurophysiological signals, which can identify the driver's braking intention earlier than the method based on driver's behavior [27], [28]. Wang and Haufe proposed a driver emergency braking intention method based on electromyography and electroencephalography (EEG), and identification results earlier than real-world driving behavior [29], [30].

Meanwhile, the driving intention is the thinking activities which cannot be observed directly. They have to be inferred from observation sequence which is composed of vehicle state (e.g., longitudinal acceleration, lateral acceleration, yaw velocity and speed), driver's characteristics (e.g., head motion, eye gaze, brain signal, body motion), and driver's operation (e.g. steering wheel angle, pedal displacement, pedal force) [23], [31], [32]. However, vehicle state belongs to post-effect data, and some parameters cannot be measured directly. Driver's characteristic data can be obtained by wearing special equipment and the movement characteristics are different in individuality, which are suitable for off-line identification.

All the above-mentioned related research can be seen that the most widely used method of driving intention identification are HMM and machine learning techniques. HMM can reflect the dynamic characteristics of driving intention in time series well. However, this method considers that the future state of the system is only related to the current state, which is a process without after-effect. But in the real world, human thoughts are not a Markov process. At the same time, the length of driver's operation observation sequence is different. The HMM usually uses a fixed time window which has great impact on recognition effect under the different time window. When there are too many hidden nodes in the model, larger time window must be chosen. And the growth of state space is related to the size of time window, which will lead to a rapid increase in computational complexity.

Although the machine learning techniques have strong classification self-learning ability among the categories, only the current time parameters are used in the driving intention identification process, and the connection between the former and the latter moment is ignored. Therefore, the dynamic characteristics of the identification are not obvious.

The Long Short-Term Memory (LSTM) model proposed by Hochreiter and Schmidhuber is an improvement of Recurrent Neural Network (RNN) [33], [34]. LSTM has a significant advantage in capturing long-range time-dependent relationships, since they cannot access long-range context due to the backpropagated error either inflating or decaying over time[35]. Although RNN is good at modeling variable-length sequence data, the hidden state of each step can contain almost arbitrarily large time window, but when the length of the sequence is longer enough, the model will appear gradient explode or vanish in the process of back propagation, which will invalidate the long time memory of RNN [36], [37].

LSTM is an effective method to solve the problem of gradient vanish by introducing the ''gating'' mechanism. It can make up for the poor effect of RNN in long time series information transmission. LSTM network has shown excellent performance in many pattern recognition fields such as language translation, image analysis, speech recognition, fault diagnosis and text recognition [38]–[41]. Because the RNN maintains its memory of hidden states over time and has feedback loops between them, it can take full advantage of the timing of the driver sequence of operations to find connections between operations and driving intention [42]. Therefore, LSTM algorithm is used in this manuscript to build the driver braking intention recognition model.

The main contribution of this study can be attributed to the following aspects: Driver braking intentions identification model based on LSTM is established based on the analysis of brake pedal operation behaviors. The suitable characteristic parameters of braking intention identification model are selected using SVM-RFE algorithm. The random search is used to optimize the hyper-parameters of LSTM.

This paper is organized as follows. The LSTM-based model and GHMM-based model which is chosen as the comparison are presented in Section 2. Test and data preprocessing are presented in Section 3. Off-line training braking intention identification model based on LSTM and GHMM model is discussed in Section 4. The online identification of braking intention identification model is presented in Section 5. Finally, Section 6 presents the conclusions of this study.
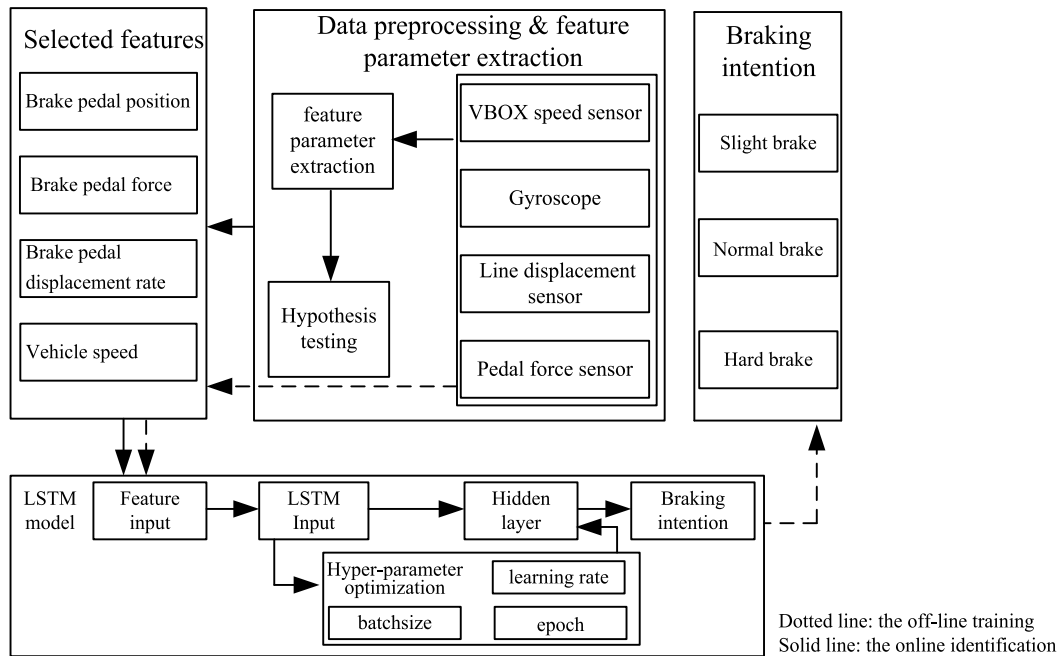
FIGURE 1. Framework of the LSTM-based driver braking intention identification model.

II. LSTM-BASED DRIVER BRAKING INTENTION IDENTIFICATION MODEL

The framework of the LSTM-based driver braking intention identification model is shown in Fig. 1.

The LSTM is a machine learning algorithm which requires a certain large amount of test data for off-line training. Thus, the real vehicle braking test was conducted. And the experiment data, such as vehicle speed, brake pedal displacement, brake pedal speed, brake pedal acceleration, brake pedal force, ect., were obtained by using VBOX speed sensor, gyroscope, line displacement sensor and pedal force sensor. The direct data and indirect data obtained by simple numerical calculation have certain correlation. In order to decrease the complexity of the model and improve the computational efficiency, the acquired parameters of these sensors were processed by feature extraction method. And brake pedal speed, vehicle speed, brake pedal displacement, and brake pedal force were determined as the characteristic parameters of the braking intention identification model. The data obtained from the test cannot be directly used to train the braking intention model. The data must be preprocessed. The de-noised and normalized characteristic parameters are taken as the input sequence of the model and the braking intention is taken as the output of the LSTM model. Although the LSTM has good generality and generalization, the setting of its hyper-parameters still has a decisive influence on its training time and model accuracy. In order to improve the learning speed and avoid model overfitting, random search is used in this manuscript to optimize the learning rate, MiniBatchsizes and MaxEpoch of the model. Thus, the driver braking intention identification model based on LSTM is established.

A. MODEL FEATURE SELECTION

The brake pedal displacement and force are chosen as the feature parameters of braking intention identification model normally. Some scholars also choose brake pedal angular velocity, brake pedal speed, and vehicle deceleration as identification parameters. The lack of feature parameters will ignore the key information of driver operation in the identification process and will lead to inaccurate description. Too many feature parameters will make the decision maker been inundating with the ocean of information and unable to make a correct judgment. At the same time, noise and redundancy features not only increase the computation time, but also may reduce the generalization ability of the model. Therefore, feature selection theory should be used to select the suitable feature parameters of the driver's braking intention identification model.

Filter, Wrapper and Embedded methods are commonly used for feature parameter selection. The advantage of the Filter method is that the time complexity is low, even for a large number of data. However, because it is relatively simple and independent of the classifier, the sample quality will have a great impact on the accuracy of statistics. While the Wrapper method is easy to overfit.

Support vector machine (SVM) is insensitive to dimension disasters and can deal with high dimension model well. At the same time, its model parameters depend on the number of samples rather than the number of features, so it can adapt to the high-dimensional small sample data well. Because of these advantages, Guyon *et al.* proposed an advanced Wrapper feature selection method that combines support vector machine (SVM) with subsequent item deletion search

strategy - recursive feature elimination method based on SVM (SVM-RFE) [43], [44].

Since each dimension of the SVM hyperplane corresponds to each feature in the data set, the dimension weight on the hyperplane can be regarded as the contribution or importance of this dimension (feature). So, weights can be used to rank features from the most important to the least important. The SVM-RFE procedure is as follows:

(1) Initially, the current feature subset Current_D contains all the features, and the optimal feature subset Best_D is null set.

(2) Set the proportion E% of the number of features to be deleted in each step.

(3) Repeat the following procedures until the feature subset Current_D is a null set.

The SVM model was established based on the current feature subset Current_D to obtain its ranking score w;

Rank the features of Current_D in descending order according to the ranking score w;

Removes E% of the features sorted at the end of the current feature subset Current_D;

(4) If the accuracy of current feature subset Current_D is higher than that of the optimal feature subset Best_D, let the optimal feature subset to be the current feature subset Current_D.

(5) Return the optimal subset of features Best_D.

In this paper, the Current_D contains vehicle speed, brake pedal displacement, brake pedal speed, brake pedal acceleration, brake pedal force, change rate of brake pedal force and rate of change of brake pedal force. The feature parameters will be selected by using pre-processed data.

B. ESTABLISHMENT OF DRIVER BRAKING INTENTION IDENTIFICATION MODEL BASED ON LSTM

As shown in Fig. 2, the braking process can be divided into three stages: (1) brake pedal pressing stage; (2) brake pedal keeping stage; (3) brake pedal releasing stage. These three stages can be further subdivided into hard brake pedal pressing stage, normal brake pedal pressing stage, slightly brake pedal pressing stage, brake pedal keeping stage, brake
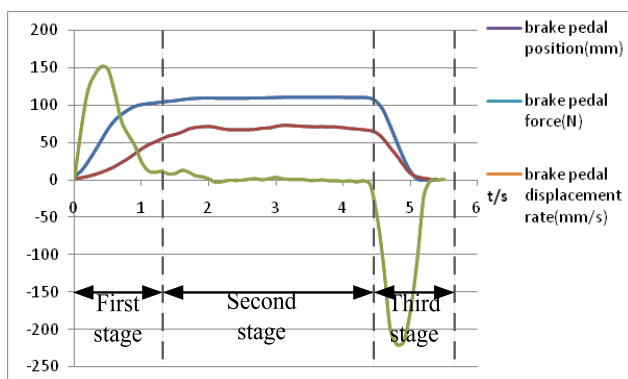

FIGURE 2. Brake pedal operation process.

pedal releasing stage. The driving intention is composed of these simple basic operations that represent the driver's behavior. For example, the hard brake intention is composed of a series of actions including hard brake pedal pressing stage, normal brake pedal pressing stage, brake pedal keeping stage and brake pedal releasing stage in a certain sequence of time. This timing feature is in line with the characteristics of LSTM algorithm. According to the result of feature selection, the input and the output of LSTM model at time t is defined as:

$$x_t = \{a(t), b(t), c(t), d(t)\} \tag{1}$$
$$h_t = \{slight\ brake, normal\ brake, hard\ brake\} \tag{2}$$

where, x_t is the input of LSTM model at time t; h_t is the output of LSTM model; $a(t)$ is the brake pedal force; $b(t)$ is the brake pedal displacement; $x(t)$ is the brake pedal acceleration; $d(t)$ is the vehicle speed.

LSTM model makes use of the structure of "gate" to transmit information selectively. The "gate" structure includes the input gate, output gate, and forget gate. And memory cells are used to realize timing memory and timing prediction. The internal structure of LSTM node is shown in Fig. 3. The construction process of driver braking intention identification model based on LSTM is as follows:

(1) Computing input gate

The input gate consists of a sigmoid layer and a tanh layer. The sigmoid layer determines what information will be updated in the memory unit. The tanh layer determines the candidate memory cell σ at current time.

$$i_t = \sigma\left(w_{ix}x_t + w_{ih}h_{t-1} + b_i\right) \tag{3}$$
$$g_t = \tanh\left(w_{gx}x_t + w_{gh}h_{t-1} + b_g\right) \tag{4}$$

where, $(w_{ix}; w_{ih}; b_i)$ is the weight matrix and bias matrix of the input gate; w_{gx} and w_{gh} are the weight matrix and bias matrix of memory units respectively, sigmod and tanh are nonlinear activation functions.

(2) Computing forget gate

The forget gate has only one sigmoid layer, which is used to determine whether information should be discarded. f = 1 means to retain all information, and f = 0 means to forget all information.

$$f_t = \sigma\left(w_{fx}x_t + w_{fh}h_{t-1} + b_f\right) \quad f \in [0, 1] \tag{5}$$

where, $(w_{fx}; w_{fh}; b_f)$ is the weight matrix and bias matrix of the forget gate.

(3) Computing output gate

The output gate determines the output information of the model according to the state of the memory unit. The first step is to use the sigmoid layer to calculate which part of the memory unit state to output. In the second step, the tanh activation function is used to process the cell state. The third step multiplies the state value by the output value of the sigmoid layer.
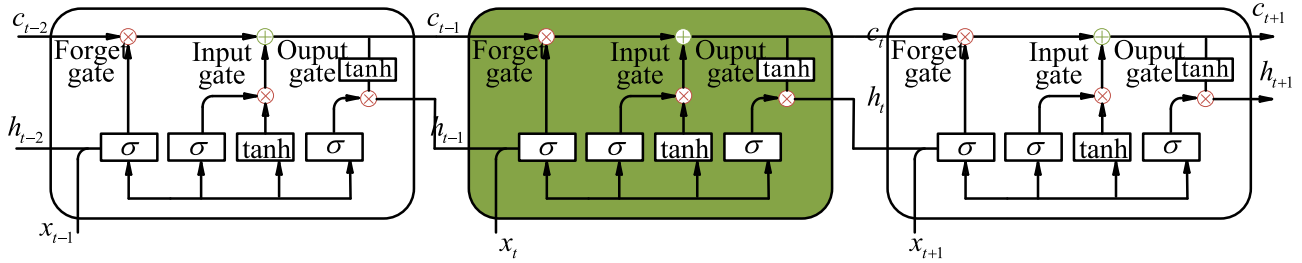
$$o_t = \sigma(w_{ox}x_t + w_{oh}h_{t-1} + b_o) \tag{6}$$

FIGURE 3. Internal structure of LSTM node.

FIGURE 4. Automobile comprehensive performance testing ground of Chang'an university.

where, $(w_{ox}; w_{oh}; b_o)$ is the weight matrix and bias matrix of the output gate.

(4) Updating the memory unit status

$$c_t = f_t c_{t-1} + i_t g_t \tag{7}$$

(5) Computing the LSTM output

$$h_t = o_t \tanh(c_t) \tag{8}$$

III. TEST AND DATA PREPROCESSING

A. TEST PLAN AND DATA COLLECTION

The real vehicle test was conducted in the automobile comprehensive performance testing ground of Chang'an university, as shown in Fig. 4. In order to eliminate the influence of driving skills on test results, three drivers with different driving experience were selected to conduct hard braking, normal braking and slight braking tests under 30km/h, 50km/h and 70km/h respectively. The test process is as follows:

① Hard braking: The test vehicle travels at a constant speed to the designated position, then the driver will perform hard braking.

② Normal braking: The test vehicle travels at a constant speed to the designated position, then the driver will perform normal braking.

③ Slight braking: The test vehicle travels at a constant speed to the designated position, then the driver will perform slight braking.

Test data distribution results are shown in table 1. The text data are divided into two parts. The $\frac{3}{4}$ test data are used for training the model, and the remaining test data are used for model verification.

TABLE 1. Test data distribution.

	30km/h	50km/h	70km/h
Hard braking	90	70	30
Normal braking	150	150	150
Slight braking	300	210	120

VBOX speed sensor, gyroscope, line displacement sensor, OBD and pedal force sensor are used to collect the vehicle speed, acceleration, brake pedal displacement, brake pedal displacement rate and brake pedal force during the test. Considering the accuracy, range, reliability and stability of sensors, the characteristics of output signals, the installation convenience and other factors, the selected sensors are shown in the table 2. And the test equipment is shown in Fig. 5. Meanwhile, in order to realize real-time and synchronous acquisition of multi-channel sensor signals, a 32-channel data acquisition instrument manufactured by Austria Co. DEWETRON, ltd. is adopted to record the signals in real time.
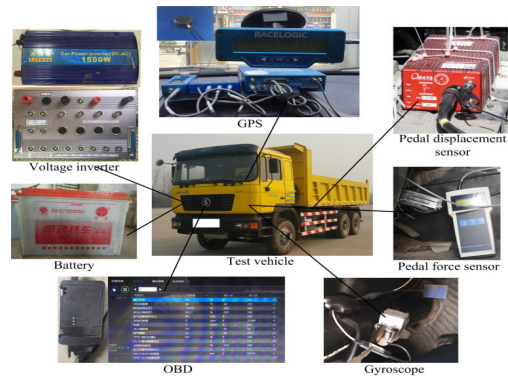

FIGURE 5. Test equipment.

B. DATA PREPROCESSING

In the ideal condition, the driver only presses or releases the pedals after intends to brake. But in reality, engine vibration, road bumps and other vibrations will also cause brake pedal jitter. Hence, whether or not the brake pedal displacement, brake pedal displacement rate and brake pedal force are equal to 0 are not appropriate conditions for identifying driver braking operations. It is necessary to determine a threshold.

In this paper, the interval estimation method is adopted to determine the threshold of non man-made boundary of brake pedal. The brake behavior data are divided into two categories: non man-made action data and man-made action

TABLE 2. Test equipment and acquisition parameters.

Test equipment	Model	Parameters or function	Accuracy	Frequency
Test vehicle	DL-3000	-	-	-
OBD	SQ1010	Speed	0.1km/h	10Hz
		Brake pedal displacement	0.1%	10Hz
		Brake pedal force	1.0%	10Hz
GPS	RLVB3iSL	Speed	0.01km/h	20Hz
Pedal displacement sensor	SENST2-631	Brake pedal displacement	0.01%	20Hz
Pedal force sensor	PKH2.0/HT2.0	Brake pedal force	0.50%	20Hz
Gyroscope	RT3100	Deceleration	0.10%	20Hz
Voltage inverter	1500w	Convert 12V to 220V	-	-
Battery	12V	Power supply	-	-

data. The man-made action data of brake pedal are selected as the final training data. Based on point estimation and sample error, interval estimation is a method in mathematical statistics to infer the range of parameters according to certain hypothesis conditions with a certain degree of confidence. The data of pedal force and pedal displacement in idling state of engine, running on flat road and running on bumpy road are collected, and the boundary of non man-made action of brake pedal can be inferred based on the test data samples by using interval estimation theory.

As the population variance of the brake pedal displacement, the brake pedal displacement change rate, and brake pedal force are unknown, for the sample $X_1, X_2, \cdots, X_n$ from X, S^2 is an unbiased estimation of σ^2, therefore[45]:

$$\frac{\overline{X} - \mu}{S/\sqrt{n}} \sim t(n-1) \tag{9}$$

And the $t(n-1)$ distribution doesn't depend on any unknown parameters. $\frac{\overline{X} - \mu}{S/\sqrt{n}}$ is chosen as the pivot.

$$P\left\{-t_{\alpha/2}(n-1) < \frac{\overline{X} - \mu}{S/\sqrt{n}} < t_{\alpha/2}(n-1)\right\} = 1 - \alpha \tag{10}$$

where, $\overline{X}$ and S^2 are the sample mean and variance of X; n is the number of samples; $t_p(n-1)$ is the p quantile of student's t-distribution in $(n-1)$ degrees of freedom; $p = 1 - \alpha/2$, and $\alpha = 0.01, p = 0.995$.

The confidence interval of the sample X at the confidence level $1 - \alpha$ can be obtained.

$$\overline{X} \pm \frac{S}{\sqrt{n}} t_{\alpha/2}(n-1) \tag{11}$$

Thus, the boundary of non man-made action of brake pedal displacement, pedal force and pedal displacement rate can be obtained from statistical data. The sampling frequency was set to 10Hz. The boundary value of brake pedal displacement obtained by interval estimation was $[-0.1773, 1.1721]$, and the boundary value of brake pedal force was $[-0.9042, 1.1422]$. The boundary thresholds are shown in Fig. 6.

Finally, in order to avoid the influence of different dimensions of parameters, the input parameters are normalized.

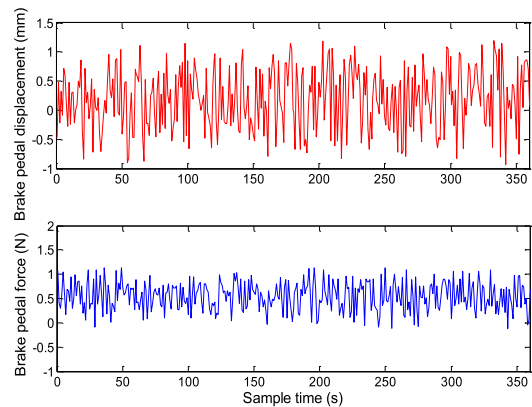$$\overline{x} = \frac{x - \min}{\max - \min} \tag{12}$$

FIGURE 6. Boundary thresholds.

C. FEATURE SELECTION

The Filtering method based on SVM-RFE is used to select the feature parameters of driver braking intention recognition. Brake pedal displacement, brake pedal speed, brake pedal acceleration, brake pedal force, change rate of brake pedal force and rate of change of brake pedal force are alternative feature parameters. The ranking score order of each feature is shown in table 3.

TABLE 3. Ranking score of alternative feature parameters.

Feature	3	1	2	5	4	6	7
weight	4.778	2.885	3.631	1.969	1.207	1.076	0.596

The ranking score order of each feature is as follows:
feature 3> feature 1> feature 2> feature 5> feature 4> feature 6> feature 7

From the first parameter to the seventh parameter, it is the vehicle speed, brake pedal displacement, brake pedal speed, brake pedal acceleration, brake pedal force, change rate of brake pedal force, and rate of change of brake pedal force. After the feature selection, feature4, feature6, feature7 are removed, so we choose vehicle speed, brake pedal displacement, brake pedal speed, brake pedal force as the characteristic parameters for braking intention identification.

IV. OFF-LINE TRAINING

A. LSTM OFF-LINE TRAINING

Although the deep neural network has good generality and generalization, the setting of its hyper-parameters still has a decisive influence on its training effect and model accuracy. In order to improve the learning speed and avoid model over-fitting, it is necessary to optimize the hyper-parameters. However, the time cost of manual adjustment of hyper-parameter is high, the results are difficult to reproduce, and may not be adjusted to the optimal results. Therefore, grid search algorithm, random search algorithm, genetic algorithm, particle swarm optimization, Bayesian optimization algorithm and other automatic optimization methods are mostly adopted at present.

Bayesian optimization is the global optimization algorithm, which assumes that the unknown function is sampled from a Gaussian process and maintains posterior distribution of the function during observation [46], [47]. Therefore, the method needs to determine the mean and variance of Gaussian distribution. Grid search and manual search are the most widely used strategies in hyper-parameter optimization. Grid search has high reliability in low-dimensional space, low technical difficulty, easy implementation and parallelization, so it is suitable for optimization with few hyper parameters. However, as the number of hyper-parameters increases, the amount of computation required for grid search increases exponentially. Random search is to extract a certain number of candidate combinations from the parameter space with specific distribution, which avoids the traversal hyper-parameter space of grid search. It is more efficient than grid search in optimizing parameters of single layer neural network classifier [48]. It not only keeps the advantages of easy implementation and high reproducible of grid search, but also achieves the small reduction of efficiency in low dimensional space in exchange for the substantial increase of efficiency in the high dimensional space. Therefore, random search is used in this manuscript to optimize the learning rate, Mini-Batchsizes and MaxEpoch of the model. The accuracy, loss and iteration times of different learning rates, MiniBatchsizes and MaxEpoch are shown in the Fig. 7. It can be seen that the model performance with optimized hyper-parameters is significantly better. After the optimization, MiniBatchsizes=22, MaxEpoch=100, and learning rate=0.011.

B. GHMM OFF-LINE TRAINING

GHMM is a common method in pattern recognition [20], [21], [49]. In order to verify the effect of the proposed method, the driver's braking intention identification model based on GHMM model is taken as a comparison model in this paper.

The 952 groups of data of brake pedal pressing stage in slight, normal and hard braking condition are chosen for offline training of the GHMM model. There are 142 groups of hard brake data, 337 groups of normal brake data, and 472 groups of slight brake data. The parameters of the GHMM model are shown as follows.

$$GHMM = \{prior, transmat, mix\{N, mixmat, Sigma, mu\}\} \quad (13)$$

where, *prior* is the initial state matrix, *transmat* is the state transition matrix, *mix* is the mixture Gaussian parameter array, *N* is the number of Gaussian function, *mixmat* is the weight of each Gaussian function in GHMM, *mu* is the mean of each Gaussian function, *Sigma* is the covariance of each Gaussian function.

The GHMM models of hard braking intention, normal braking intention and slow braking intention were trained under the time window of 0.5s, 1s,2s and 3s respectively. The parameters of the hard braking under the time window of 1s are shown as follows:

$$N = 3, \quad prior = \begin{bmatrix} 0 & 1 & 1.2442 \times 10^{-72} \end{bmatrix},$$

$$transmat = \begin{bmatrix} 0.8838 & 0.1025 & 0.0137 \\ 0 & 0.1 & 0.9 \\ 0.18 & 4.2922 \times 10^{-77} & 0.82 \end{bmatrix},$$

$$mu = \begin{bmatrix} 154.5785 & 3.1578 & 135.1065 \\ 273.2089 & 1.0880 & 144.6540 \\ 20.1633 & 30.8594 & 46.2839 \end{bmatrix},$$

$$mix = \{mix\{1\} \ mix\{2\} \ mix\{3\}\},$$

$$mix\{1\}.mixmat = [0.0126 0.9621 0.0253],$$

$$mix\{1\}.Sigma = [val(:,:,1) \ val(:,:,1) \ val(:,:,1)]$$

V. ONLINE IDENTIFICATION

A. GHMM MODEL ONLINE IDENTIFICATION

The 48 groups of hard braking data, 113 groups of normal braking data and 158 groups of slight braking data are selected to make GHMM online recognition. Meanwhile, 0.5s, 1s, 2s and 3s are selected as time windows for driver's braking intention identification, respectively. The accuracy of GHMM models with different time windows is shown in table 4. The identification results of three braking intentions under different time windows are shown in Fig. 8-10. The identification results of the three GHMM are expressed by 50, 100, 150, respectively.

For different braking intention identification models with different time windows, there are significant differences in the model accuracy. When the time windows are 1s, 2s and 3s of hard braking intention, the accuracy reaches 100%. And when the time window is 0.5s, it reaches 100%. The difference is not obvious. Under normal braking intention, the highest accuracy rate is 90.0684% when the time window is 1s, and the lowest is 85.1851% when the time window is 3s, with a difference of 5.968%. Under slight braking intention, the highest accuracy rate is 88.2877% when the time window is 1s, and the lowest is 79.0645% when the time window is 0.5s, with a difference of 9.2232%. It can be seen that the size of time window has a significant impact on the accuracy of model identification in the two braking intentions. Meanwhile, only four sizes of time window have been used
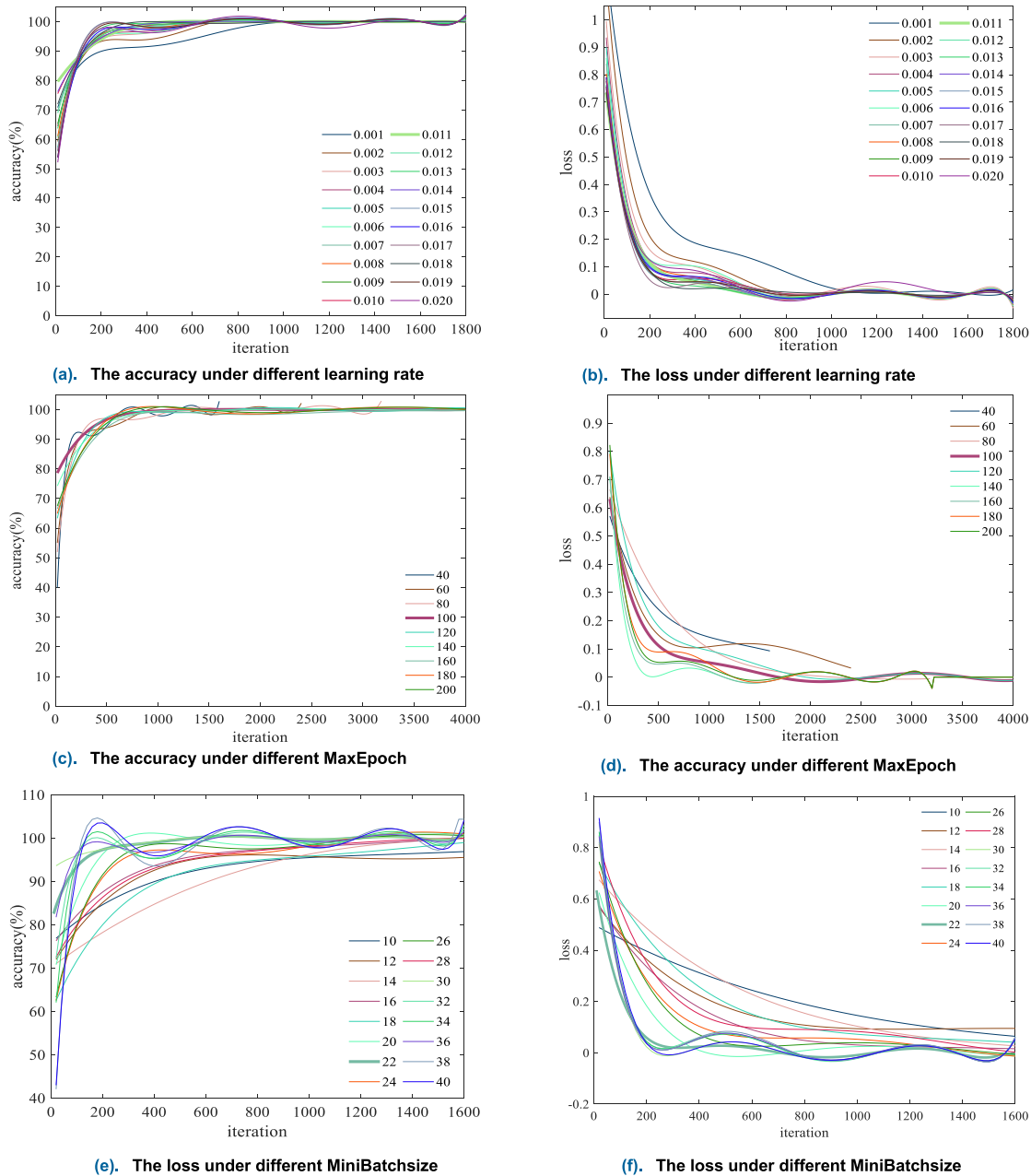
(a). The accuracy under different learning rate

(b). The loss under different learning rate

(c). The accuracy under different MaxEpoch

(d). The accuracy under different MaxEpoch

(e). The loss under different MiniBatchsize

(f). The loss under different MiniBatchsize

FIGURE 7. (a) The accuracy under different learning rate. (b) The loss under different learning rate. (c) The accuracy under different MaxEpoch. (d) The accuracy under different MaxEpoch. (e) The loss under different MiniBatchsize. (f) The loss under different MiniBatchsize.

in this paper, which cannot indicate that the time window of 1s for slight braking intention and the time window of 1s for normal braking intention is optimal and can achieve the highest accuracy.

The identification result of the normal braking intention under different time windows is shown in the Fig. 8. When the time window is 0.5s, it is mistakenly identified as hard braking at 0.1-0.2s and slow braking at 0.3s. When the time window is 1s, normal braking intention is mistakenly identified as slight braking at 1.1-1.2s and 2.7-2.9s. When the time window is 2s, normal braking intention is mistakenly

identified as hard braking at 0.3-0.5s, and slow braking at 1.01-1.2s. When the time window is 3s, normal braking intention is mistakenly identified as slight braking at 0.1-0.4s.

The identification result of the slight braking intention under different time windows is shown in the Fig. 9. When the time window is 0.5s, it is mistakenly identified as normal braking at 0.9-1.6s. When the time window is 1s, it is mistakenly identified as normal braking at 0.6-1.5s. When the time window is 2s, it is mistakenly identified as normal braking at 0.1-0.7s. However, when the time window is 3s, there is no mistaken identification.

TABLE 4. Accuracy of different driving intention identification models with different time windows.

Braking intention / Time window	Hard braking	Normal braking	Slight braking
0.5s	98.4402	85.1851	79.0645
1s	100	90.0684	88.2877
2s	100	84.7272	82.6083
3s	100	84.0968	83.4839
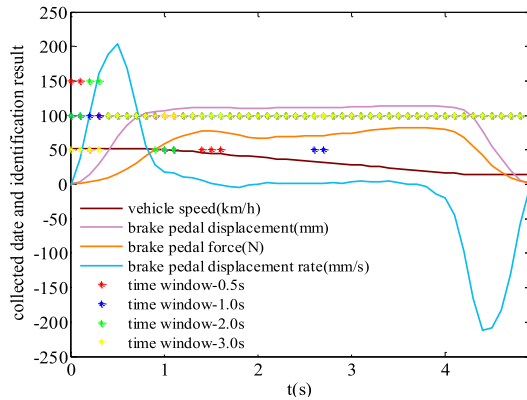
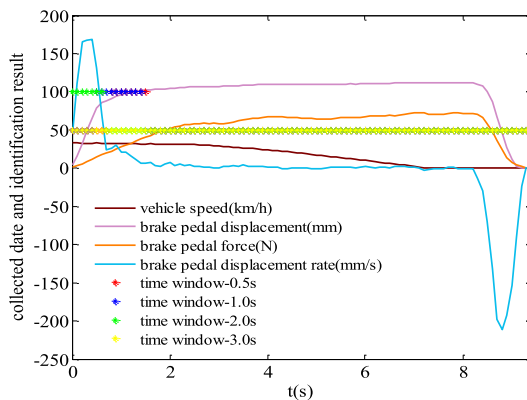**FIGURE 8.** The identification result of the normal braking intention under different time windows.

FIGURE 9. The identification result of the slight braking intention under different time windows.

Through the above comparison, it can be seen that the time points and types of mistake are random in every braking intention under different time windows. Therefore, the optimal time window of each model is not the same. The optimal time window can improve the identification accuracy of driving intention, but the selection of optimal time window will increase the workload of the model.

B. LSTM MODEL ONLINE IDENTIFICATION

The data which are same to GHMM recognition are selected. These data are used to make LSTM model online recognition. The accuracy of model identification with different MiniBatchsizes, MaxEpoch and learning rate is shown in the Fig. 11. The maximum, minimum, first quartile, median, third quartile of the accuracy are shown in table 5.

It can be seen from the table 5 that under different hyper-parameters, the maximum accuracy difference is 48.64%, and
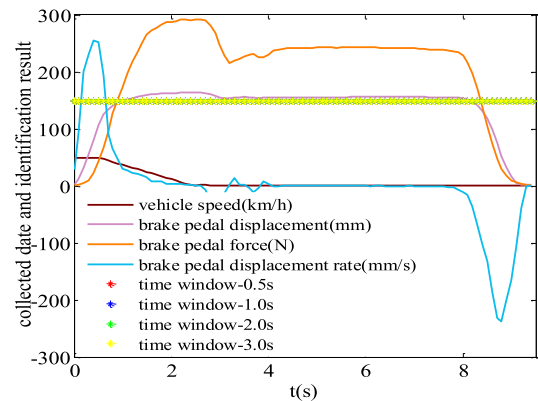

FIGURE 10. The identification result of the hard braking intention under different time windows.
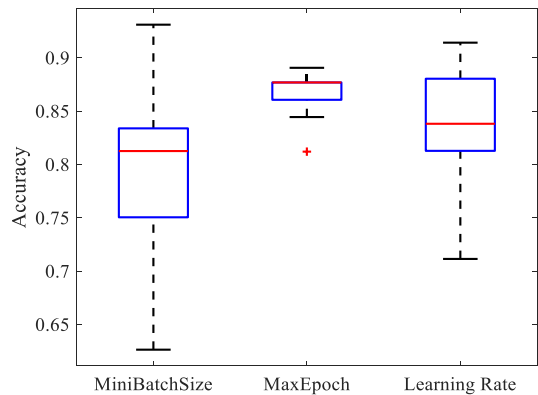

FIGURE 11. Boxplot of the LSTM model identification result.

the minimum accuracy difference is 9.67%. The quartiles further demonstrate the influence of different hyper-parameters on the identification accuracy. And the model accuracy is also optimized by hyper-parameter optimizing.

In order to further verify the effect of driver braking intention recognition model proposed in this paper, the accuracy, recall, Precision, F-measure of the braking intention identification model based on LSTM and based on GHMM are compared. The confusion matrixes of the LSTM-based and GHMM-based model are shown in the table 6.

From table 6, it can be seen that the Precision, Recall, F-measure, Accuracy of the braking intention identification model proposed in this paper based on LSTM are better than that of the braking intention identification model based on GHMM. In particular, the evaluation index of LSTM-based normal braking intention and slow braking intention identification model are obviously better than the GHMM-based model. The thermodynamic diagram of confusion matrixes of the LSTM-based and GHMM-based model is shown in Fig. 12. Through comparison, it can be seen that under the premise of improving the fitting ability, the braking intention identification model based on LSTM model did not lead to over-fitting phenomenon, and effectively mined the potential feature information of the data set. Moreover, the recall and accuracy of the LSTM-based braking intention identification models are above 0.95, indicating the good ability of intention identification.

TABLE 5. The maximum, minimum, first quartile, median, third quartile of the accuracy.

Parameter	minimum	first quartile	median	third quartile	maximum
Mini batchsize	0.62631	0.75042	0.81252	0.8338	0.931
Max Epoch	0.811972	0.86057	0.876832	0.876832	0.89057
Learning rate	0.711382	0.829668	0.846524	0.880334	0.914144

TABLE 6. The accuracy, recall, Precision, F-measure of the braking intention identification model.

Evaluation index		Precision		Recall		F-measure		Accuracy	
		LSTM	GHMM	LSTM	GHMM	LSTM	GHMM	LSTM	GHMM
Intention	Slight braking	0.967	0.939	0.955	0.886	0.961	0.912	0.962	0.915
	Normal braking	0.939	0.790	0.955	0.902	0.947	0.842	0.962	0.880
	Hard braking	1	0.96	1	1	1	0.979	1	0.993
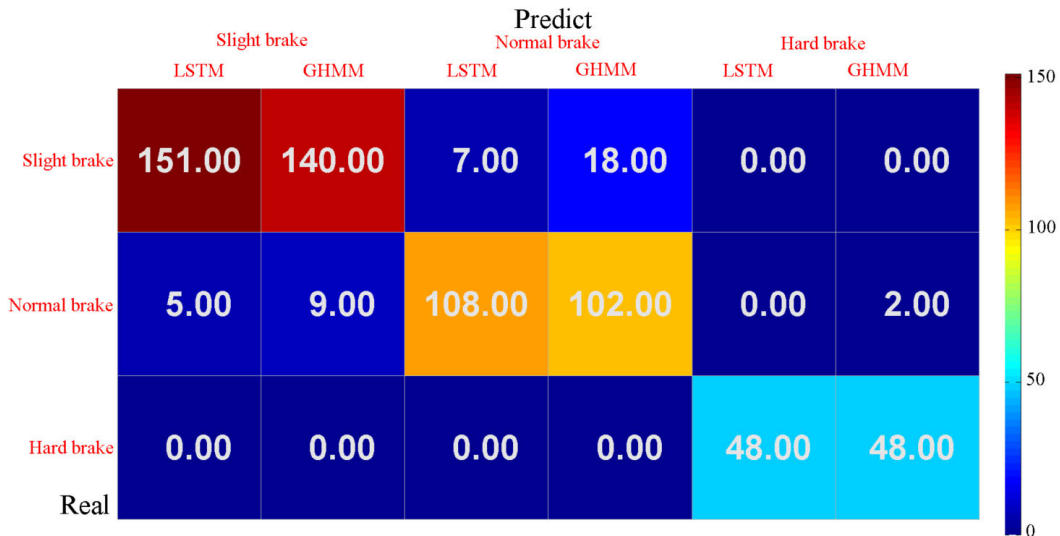
FIGURE 12. The thermodynamic diagram of confusion matrixes of the LSTM-based and GHMM-based model.

VI. CONCLUSION

(1) Driver braking intentions identification model based on LSTM is established based on experiment data and the analysis of brake pedal operation behaviors. SVM-RFE algorithm is used to select the characteristic parameters of braking intention identification model. LSTM models are trained offline and recognized online. The random search is subsequently used to optimize the hyper-parameters of LSTM. The results show that the Recall and Accuracy of the LSTM-based braking intention identification models are above 0.95. The model has good real-time performance and accuracy.

(2) In further research, the braking intention prediction model will be studied on the basis of braking intention identification model. The predictive braking intention can be used to control the vehicle braking system in advance, which will improve the safety and comfort of the vehicle and the braking energy recovery efficiency of the electric vehicle. At the same time, this method can not only be used to construct the braking intention identification model but also can be used to construct the acceleration, steering, lane change and other complex driving intention identification models. Also, gradient explosion problem has been solved in LSTM to some extent, but not completely. The order of magnitude of time sequence information which LSTM can process is limited. Since each cell has four full connection layers (MLP), if the time span of LSTM is large and the network is deep, the calculation amount will increase rapidly. These are also the problems that need to be addressed in future research.

REFERENCES

[1] J. Bärgman, C.-N. Boda, and M. Dozza, "Counterfactual simulations applied to SHRP2 crashes: The effect of driver behavior models on safety benefit estimations of intelligent safety systems," *Accident Anal. Prevention*, vol. 102, pp. 165–180, May 2017, doi: 10.1016/j.aap.2017.03.003.

[2] X. Zhao, X. Zhao, Q. Yu, Y. Ye, and M. Yu, "Development of a representative urban driving cycle construction methodology for electric vehicles: A case study in Xi'an," *Transp. Res. D, Transp. Environ.*, vol. 81, Apr. 2020, Art. no. 102279, doi: 10.1016/j.trd.2020.102279.

[3] H. K. Lee, S. G. Shin, and D. S. Kwon, "Design of emergency braking algorithm for pedestrian protection based on multisensor fusion," *Int. J. Automot. Technol.*, vol. 18, no. 6, pp. 1067–1076, 2017, doi: 10.1007/s12239-017-0104-7.

[4] J. Duan, R. Li, L. Hou, W. Wang, G. Li, S. E. Li, B. Cheng, and H. Gao, "Driver braking behavior analysis to improve autonomous emergency braking systems in typical Chinese vehicle-bicycle conflicts," *Accident Anal. Prevention*, vol. 108, pp. 74–82, Nov. 2017, doi: 10.1016/j.aap.2017.08.022.

[5] T. Imamura, T. Ogi, Z. Zhang, and T. Miyake, "Study of induction and estimation method for Driver's intention by using a driving simulator," in *Proc. IEEE Int. Conf. Syst., Man, Cybern.*, Oct. 2013, pp. 3322–3326, doi: 10.1109/SMC.2013.566.

[6] J. B. Cicchino, "Effectiveness of forward collision warning and autonomous emergency braking systems in reducing front-to-rear crash rates," *Accident Anal. Prevention*, vol. 99, pp. 142–152, Feb. 2017, doi: 10.1016/j.aap.2016.11.009.

[7] I. Isaksson-Hellman and M. Lindman, "Evaluation of the crash mitigation effect of low-speed automated emergency braking systems based on insurance claims data," *Traffic Injury Prevention*, vol. 17, no. 1, pp. 42–47, Sep. 2016, doi: 10.1080/15389588.2016.1186802.

[8] D. Zhao, L. Chu, N. Xu, C. Sun, Y. and Xu, "Development of a cooperative braking system for front-wheel drive electric vehicles," *Energies*, vol. 11, no. 2, pp. 378–401, 2018, doi: 10.3390/en11020378.

[9] J. Ko, S. Ko, H. Son, B. Yoo, J. Cheon, and H. Kim, "Development of brake system and regenerative braking cooperative control algorithm for automatic-transmission-based hybrid electric vehicles," *IEEE Trans. Veh. Technol.*, vol. 64, no. 2, pp. 431–440, Feb. 2015, doi: 10.1109/TVT.2014.2325056.

[10] H. Liu, W. Deng, R. He, J. Wu, and B. Zhu, "Function-based architecture design for next-generation automotive brake controls," *SAE Int. J. Passenger Cars Mech. Syst.*, vol. 9, no. 1, pp. 135–142, Apr. 2016, doi: 10.4271/2016-01-0467.

[11] Y. Luo, Y. Han, L. Chen, and K. Li, "Downhill safety assistance control for hybrid electric vehicles based on the downhill driver's intention model," *Proc. Inst. Mech. Eng., D, J. Automobile Eng.*, vol. 229, no. 13, pp. 1848–1860, Nov. 2015, doi: 10.1177/0954407014567908.

[12] W. Li, H. Du, and W. Li, "A new torque distribution strategy for blended anti-lock braking systems of electric vehicles based on road conditions and Driver's intentions," *SAE Int. J. Passenger Cars Mech. Syst.*, vol. 9, no. 1, pp. 107–115, Apr. 2016, doi: 10.4271/2016-01-0461.

[13] G. Xu, W. Li, K. Xu, and Z. Song, "An intelligent regenerative braking strategy for electric vehicles," *Energies*, vol. 4, no. 9, pp. 1461–1477, Sep. 2011, doi: 10.3390/en4091461.

[14] J. Ruan, P. D. Walker, P. A. Watterson, and N. Zhang, "The dynamic performance and economic benefit of a blended braking system in a multi-speed battery electric vehicle," *Appl. Energy*, vol. 183, pp. 1240–1258, Dec. 2016, doi: 10.1016/j.apenergy.2016.09.057.

[15] X. Zhao, S. Xu, Y. Ye, M. Yu, and G. Wang, "Composite braking AMT shift strategy for extended-range heavy commercial electric vehicle based on LHMM/ANFIS braking intention identification," *Cluster Comput.*, vol. 22, no. 4, pp. 1–16, 2018, doi: 10.1007/s10586-018-1888-6.

[16] A. Pentland and A. Liu, *Modeling and Prediction of Human Behavior*. Cambridge, MA, USA: MIT Press, 1999.

[17] N. Oliver and A. P. Pentland, "Graphical models for driver behavior recognition in a SmartCar," in *Proc. IEEE Intell. Vehicles Symp.*, Oct. 2000, pp. 7–12, doi: 10.1109/IVS.2000.898310.

[18] D. Tran, W. Sheng, L. Liu, and M. Liu, "A hidden Markov model based driver intention prediction system," in *Proc. IEEE Int. Conf. Cyber Technol. Autom., Control, Intell. Syst. (CYBER)*, Jun. 2015, pp. 115–120, doi: 10.1109/CYBER.2015.7287920.

[19] K. Li, X. Wang, Y. Xu, and J. Wang, "Lane changing intention recognition based on speech recognition models," *Transp. Res. C, Emerg. Technol.*, vol. 69, pp. 497–514, Aug. 2016, doi: 10.1016/j.trc.2015.11.007.

[20] X. Zhao, S. Wang, J. Ma, Q. Yu, Q. Gao, and M. Yu, "Identification of driver's braking intention based on a hybrid model of GHMM and GGAP-RBFNN," *Neural Comput. Appl.*, vol. 31, no. S1, pp. 161–174, Jan. 2019, doi: 10.1007/s00521-018-3672-1.

[21] S. Wang, Q. Yu, and X. Zhao, "Study on driver's turning intention recognition hybrid model of GHMM and GGAP-RBF neural network," *Adv. Mech. Eng.*, vol. 10, no. 3, Mar. 2018, Art. no. 168781401876498.

[22] J. Peng, Y. Guo, R. Fu, W. Yuan, and C. Wang, "Multi-parameter prediction of drivers' lane-changing behaviour with neural network model," *Appl. Ergonom.*, vol. 50, pp. 207–217, Sep. 2015, doi: 10.1016/j.apergo.2015.03.017.

[23] Y. Hua, H. Jiang, H. Tian, X. Xu, and L. Chen, "A comparative study of clustering analysis method for driver's steering intention classification and identification under different typical conditions," *Appl. Sci.*, vol. 7, no. 10, p. 1014, Sep. 2017, doi: 10.3390/app7101014.

[24] L. Li, Z. Zhu, X. Wang, Y. Yang, C. Yang, and J. Song, "Identification of a driver's starting intention based on an artificial neural network for vehicles equipped with an automated manual transmission," *Proc. Inst. Mech. Eng., D, J. Automobile Eng.*, vol. 230, no. 10, pp. 1417–1429, Sep. 2016, doi: 10.1177/0954407015611294.

[25] I.-H. Kim, J.-H. Bong, J. Park, and S. Park, "Prediction of driver's intention of lane change by augmenting sensor information using machine learning techniques," *Sensors*, vol. 17, no. 6, p. 1350, Jun. 2017, doi: 10.3390/s17061350.

[26] F. Bocklisch, S. F. Bocklisch, M. Beggiato, and J. F. Krems, "Adaptive fuzzy pattern classification for the online detection of driver lane change intention," *Neurocomputing*, vol. 262, pp. 148–158, Nov. 2017, doi: 10.1016/j.neucom.2017.02.089.

[27] J.-W. Kim, I.-H. Kim, and S.-W. Lee, "Detection of braking intention during simulated driving based on EEG analysis: Online study," in *Proc. IEEE Int. Conf. Syst., Man, Cybern.*, Oct. 2015, pp. 887–891, doi: 10.1109/SMC.2015.163.

[28] I.-H. Kim, J.-W. Kim, S. Haufe, and S.-W. Lee, "Detection of braking intention in diverse situations during simulated driving based on EEG feature combination," *J. Neural Eng.*, vol. 12, no. 1, Feb. 2015, Art. no. 016001, doi: 10.1088/1741-2560/12/1/016001.

[29] H. Wang, L. Bi, and T. Teng, "EEG-based emergency braking intention prediction for brain-controlled driving considering one electrode falling-off," in *Proc. 39th Annu. Int. Conf. IEEE Eng. Med. Biol. Soc. (EMBC)*, Jul. 2017, pp. 2494–2497, doi: 10.1109/EMBC.2017.8037363.

[30] S. Haufe, J.-W. Kim, I.-H. Kim, A. Sonnleitner, M. Schrauf, G. Curio, and B. Blankertz, "Electrophysiology-based detection of emergency braking intention in real-world driving," *J. Neural Eng.*, vol. 11, no. 5, Oct. 2014, Art. no. 056011, doi: 10.1088/1741-2560/11/5/056011.

[31] L. Bi, C. Wang, X. Yang, M. Wang, and Y. Liu, "Detecting driver normal and emergency lane-changing intentions with queuing network-based driver models," *Int. J. Hum.-Comput. Interact.*, 2015, vol. 31, no. 2, pp. 139–145, doi: 10.1080/10447318.2014.986638.

[32] C. Rodemerk, H. Winner, and R. Kastner, "Predicting the driver's turn intentions at urban intersections using context-based indicators," in *Proc. Intell. Vehicles Symp.*, Jun. 2015, pp. 964–969, doi: 10.1109/IVS.2015.7225809.

[33] Z. Huang, F. Ren, M. Hu, and J. Liu, "A real-time expression Mimicking method for humanoid robot based on dual LSTM fusion," *Robot*, vol. 41, no. 2, pp. 137–146, 2019.

[34] A. Graves, "Long short-term memory," in *Supervised Sequence Labelling With Recurrent Neural Networks*. Berlin, Germany: Springer, 2012, pp. 1735–1780.

[35] Y. Bengio, P. Simard, and P. Frasconi, "Learning long-term dependencies with gradient descent is difficult," *IEEE Trans. Neural Netw.*, vol. 5, no. 2, pp. 157–166, Mar. 1994.

[36] J. Long, S. Zhang, and C. Li, "Evolving deep echo state networks for intelligent fault diagnosis," *IEEE Trans. Ind. Informat.*, vol. 16, no. 7, pp. 4928–4937, Jul. 2020.

[37] J. Long, Z. Sun, C. Li, Y. Hong, Y. Bai, and S. Zhang, "A novel sparse echo autoencoder network for data-driven fault diagnosis of delta 3-D printers," *IEEE Trans. Instrum. Meas.*, vol. 69, no. 3, pp. 683–692, Mar. 2020.

[38] M. Wollmer, F. Eyben, J. Keshet, A. Graves, B. Schuller, and G. Rigoll, "Robust discriminative keyword spotting for emotionally colored spontaneous speech using bidirectional LSTM networks," in *Proc. IEEE Int. Conf. Acoust., Speech Signal Process.*, Apr. 2009, pp. 3949–3952.

[39] S. Ding, S. Qu, Y. Xi, and S. Wan, "Stimulus-driven and concept-driven analysis for image caption generation," *Neurocomputing*, vol. 398, pp. 520–530, Jul. 2020.

[40] S. Ding, S. Qu, Y. Xi, and S. Wan, "A long video caption generation algorithm for big video data retrieval," *Future Gener. Comput. Syst.*, vol. 93, pp. 583–595, Apr. 2019.

[41] S. Wan, X. Xu, T. Wang, and Z. Gu, "An intelligent video analysis method for abnormal event detection in intelligent transportation systems," *IEEE Trans. Intell. Transp. Syst.*, early access, doi: 10.1109/TITS.2020.3017505.

[42] S. Q. Nie, *Research on Modeling Discretionary Lane-Changing Behavior of Vehicles in Freeway*. Nanjing, China: Southeast Univ., 2017.

[43] K.-B. Duan, J. C. Rajapakse, H. Wang, and F. Azuaje, "Multiple SVM-RFE for gene selection in cancer classification with expression data," *IEEE Trans. Nanobiosci.*, vol. 4, no. 3, pp. 228–234, Sep. 2005.

[44] P. A. Mundra and J. C. Rajapakse, "SVM-RFE with MRMR filter for gene selection," *IEEE Trans. Nanobiosci.*, vol. 9, no. 1, pp. 31–37, Mar. 2010.

[45] Z. Sheng, S. Q. Xie, and C. Y. Pan, *Probability Theory & Mathematical Statistics*, 4th ed. Beijing, China: Higher Education Press, 2008.

[46] D. R. Jones, "A taxonomy of global optimization methods based on response surfaces," *J. Global Optim.*, vol. 21, no. 4, pp. 345–383, 2001.

[47] J. Snoek, H. Larochelle, and R. P. Adams, "Practical Bayesian optimization of machine learning algorithms," in *Proc. Adv. Neural Inf. Process. Syst.*, 2012, pp. 2951–2959.

[48] J. Bergstra and Y. Bengio, "Random search for hyper-parameter optimization," *J. Mach. Learn. Res.*, vol. 13, no. 1, pp. 281–305, 2012.

[49] S. Wang, X. Zhao, and Q. Yu, "Vehicle stability control strategy based on recognition of driver turning intention for dual-motor drive electric vehicle," *Math. Problems Eng.*, vol. 2020, pp. 1–18, Jan. 2020.

● ● ●